

Gravitomagnetism and galaxy rotation curves: a cautionary tale

A.N. Lasenby,^{1,2,*} M.P. Hobson,^{1,†} and W.E.V. Barker^{1,2,‡}

¹*Astrophysics Group, Cavendish Laboratory, JJ Thomson Avenue, Cambridge CB3 0HE, UK*

²*Kavli Institute for Cosmology, Madingley Road, Cambridge CB3 0HA, UK*

We investigate recent claims that gravitomagnetic effects in linearised general relativity can explain flat and rising rotation curves, such as those observed in galaxies, without the need for dark matter. If one models a galaxy as an axisymmetric, stationary, rotating, non-relativistic and pressureless ‘dust’ of stars in the gravitoelectromagnetic (GEM) formalism, we show that gravitomagnetic effects on the circular velocity v of a star are $O(10^{-6})$ smaller than the standard Newtonian (gravitoelectric) effects and thus any modification of galaxy rotation curves must be negligible, as might be expected. Moreover, we find that gravitomagnetic effects are $O(10^{-6})$ too small to provide the vertical support necessary to maintain the dynamical equilibrium assumed in such a model. These issues are obscured if one constructs a single equation for v , as considered previously. We nevertheless solve this equation for a galaxy having a Miyamoto–Nagai density profile since this allows for both an exact numerical integration and an accurate analytic approximation. We show that for the values of the mass, M , and semi-major and semi-minor axes, a and b , typical for a dwarf galaxy, the rotation curve depends only very weakly on M , and becomes independent of it for larger M values. Moreover, for aspect ratios $a/b > 2$, the rotation curves are concave over their entire range, which does not match observations in any galaxy. Most importantly, we show that for the poloidal gravitomagnetic flux ψ to provide the necessary vertical support, it must become singular at the origin and have extremely large values near to it. This originates from the unwitting, but forbidden, inclusion of free-space solutions of the Poisson-like equation that determines ψ and also clearly contradicts the linearised treatment implicit in the GEM formalism, hence ruling out the methodology in the form used as a means of explaining flat galaxy rotation curves. We further show that recent deliberate attempts to leverage such free-space solutions against the rotation curve problem yield no deterministic modification outside the thin disk approximation, and that, in any case, the homogeneous contributions to ψ are ruled out by the boundary value problem posed by any physical axisymmetric galaxy.

PACS numbers: 04.50.Kd, 04.60.-m, 04.20.Fy, 98.80.-k

I. INTRODUCTION

It is widely accepted that the modelling of galaxy rotation curves in general relativity (GR) requires the inclusion of a dark matter halo in order to reproduce observations [1–4]. In particular, the modelling of the approximately flat rotation curves observed in the outskirts of large spiral galaxies and, to a lesser extent, the rising rotation curves observed in smaller dwarf galaxies [5–9] is considered to pose a significant challenge to GR without such a component. The absence of any direct experimental evidence for dark matter [10] has thus led to the consideration of various modified gravity theories to attempt to explain the astrophysical data.

There are a number of claims in the literature, however, that such modifications are unnecessary since hitherto neglected effects in GR itself are capable of explaining rotation curves without dark matter. These include gravitoelectric flux confinement arising from graviton self-interaction [11–18], non-linear GR effects arising even in the weak-gravity regime [19] and, most recently, gravitomagnetic effects in linearised GR [20]. Certain elements of [20] are further developed in [21] where (although the dark matter paradigm is not directly challenged) significant gravitomagnetic corrections to the rotation curve of a toy-model galactic baryon profile are suggested. An

immediate question regarding such claims is how such significant behaviours can have been consistently missed in the long history of numerical relativity [22, 23], or in the well-developed post-Newtonian formalism [24, 25]. Perhaps unsurprisingly therefore, the claims in [11–18] and [19] have been subsequently shown to be non-viable in [26] and [27], respectively. The purpose of this paper is to perform the same function for the claims in [20, 21], by showing that gravitomagnetism in the form used therein cannot be a significant factor in explaining flat or rising galaxy rotation curves without dark matter.

Our findings concur with the recent results reported in [28], where the gravitoelectromagnetic (GEM) formulation of linearised GR was used to predict galaxy rotation curves that at all radii differ from those of Newtonian theory at the order of only $v^2/c^2 \approx 10^{-6}$, as one might expect. The main focus of the present paper, however, is to clarify *why* the approach adopted in [20] leads to such different, unexpected and incorrect results, which is not addressed in [28]. We will observe in particular the accidental involvement in [20] of homogeneous solutions to the GEM field equations: this leads us naturally to [21], where such solutions are actively employed. We will show however that such solutions do not yield any deterministic phenomenology according to the suggested approximation in [21], and that they are moreover absolutely ruled out by the absence of suitable GEM boundary conditions in the galactic environment.

The remainder of this paper is arranged as follows. In Section II, we briefly outline linearised GR, focussing on station-

* a.n.lasenby@mrao.cam.ac.uk

† mph@mrao.cam.ac.uk

‡ wb263@cam.ac.uk

ary non-relativistic matter sources, and discuss its expression in the GEM formalism in Section III. We then summarise in Section IV the application of the GEM formalism to the modelling of galaxy rotation curves, as proposed in [20]. We lay out the problems with this modelling approach in Section V. Our analysis reveals the unwitting use of homogeneous solutions to the GEM field equations. In Section VI we finally address the deliberate use in [21] of such solutions. Conclusions follow in Section VII.

II. LINEARISED GENERAL RELATIVITY

In the weak gravitational field limit appropriate for modelling galaxy rotation curves, there exist quasi-Minkowskian coordinate systems $x^\mu = (ct, x^i)$ in which the spacetime metric takes the form $g_{\mu\nu} = \eta_{\mu\nu} + h_{\mu\nu}$ where $|h_{\mu\nu}| \ll 1$ and the first and higher partial derivatives of $h_{\mu\nu}$ are also small.¹ One can conveniently reinterpret $h_{\mu\nu}$ simply as a special-relativistic symmetric rank-2 tensor field that represents the weak gravitational field on a Minkowski background spacetime and possesses the gauge freedom $h_{\mu\nu} \rightarrow h_{\mu\nu} - \partial_\mu \xi_\nu - \partial_\nu \xi_\mu$. Imposing the Lorenz gauge condition $\partial_\rho \bar{h}^{\mu\rho} = 0$ on the trace-reverse $\bar{h}_{\mu\nu} \equiv h_{\mu\nu} - \frac{1}{2}\eta_{\mu\nu}h$, where $h = \eta_{\mu\nu}h^{\mu\nu}$, the linearised GR field equations reduce to the simple form

$$\square^2 \bar{h}^{\mu\nu} = -2\kappa T^{\mu\nu}, \quad (1)$$

where $\square^2 \equiv \eta^{\mu\nu}\partial_\mu\partial_\nu$ is the d'Alembertian operator, $\kappa = 8\pi G/c^4$ is Einstein's gravitational constant and $T^{\mu\nu}$ is the matter energy-momentum tensor.

For modelling galaxy rotation curves, it is sufficient to a very good approximation to limit one's considerations to stationary, non-relativistic, perfect fluid matter sources. In this case, $\partial_0 T^{\mu\nu} = 0$ and the coordinate 3-speed u of any constituent particle is small enough compared with c that one may neglect terms of order u^2/c^2 and higher in $T^{\mu\nu}$; in particular one may take $\gamma_u = (1 - u^2/c^2)^{-1/2} \approx 1$. Moreover, the fluid pressure p is everywhere much smaller than the energy density and may thus be neglected as a source for the gravitational field. Finally, we note that $|T^{ij}|/|T^{00}| \sim u^2/c^2$ and so one should take $T^{ij} \approx 0$ to the order of our approximation. Thus, for a stationary, non-relativistic source, one approximates its energy-momentum tensor as

$$T^{00} \approx \rho c^2, \quad T^{i0} \approx c\rho u^i, \quad T^{ij} \approx 0, \quad (2)$$

where $\rho(\mathbf{x})$ is the proper-density distribution of the source and \mathbf{x} denotes a spatial 3-vector. As an immediate consequence, the particular integral of (1) yields $\bar{h}^{ij} \approx 0$. Indeed, this is consistent with the Lorenz gauge condition, which implies that

$\partial_j \bar{h}^{ij} = -\partial_0 \bar{h}^{i0}$, where the right-hand side vanishes for stationary systems. Thus, only the \bar{h}^{00} and $\bar{h}^{0i} = \bar{h}^{i0}$ components of the gravitational field tensor are non-zero in this approximation.

In linearised GR, there is an inconsistency between the field equations (1) and the equations of motion for matter in a gravitational field. From (1), one quickly finds that $\partial_\mu T^{\mu\nu} = 0$, which should be contrasted with the requirement from the full GR field equations that the covariant divergence should vanish, $\nabla_\mu T^{\mu\nu} = 0$. The latter requirement leads directly to the geodesic equation of motion for the worldline $x^\mu(\tau)$ of a test particle, namely

$$\ddot{x}^\mu + \Gamma^\mu_{\nu\sigma} \dot{x}^\nu \dot{x}^\sigma = 0, \quad (3)$$

where the dots denote differentiation with respect to the proper time τ , whereas the former requirement leads to the equation of motion $\ddot{x}^\mu = 0$. This means that the gravitational field has *no effect* on the motion of the particle and so clearly contradicts the geodesic postulate. Despite this inconsistency, one may show that the effect of weak gravitational fields on test particles may still be computed by inserting the linearised connection coefficients into the geodesic equations (3).

III. GRAVITOELECTROMAGNETISM

Gravitoelectromagnetism (GEM) provides a useful and notionally-familiar formalism for linearised GR by drawing a close analogy with classical electromagnetism (EM). Indeed, GEM is ideally suited to modelling galaxy rotation curves, since the assumption of a stationary, non-relativistic matter source leads to GEM field equations and a GEM 'Lorentz' force law (derived below) that are fully consistent and have forms analogous to their counterparts in EM; this is not possible for more general time-dependent scenarios.

The GEM formalism for linear GR with a stationary, non-relativistic source is based on the simple ansatz of relabelling² the four independent non-zero components of $\bar{h}^{\mu\nu}$ as $\bar{h}^{00} \equiv 4\Phi/c^2$ and $\bar{h}^{0i} \equiv A^i/c$, where we have defined the gravitational scalar potential Φ and spatial gravitomagnetic vector potential A^i . On lowering indices, the corresponding components of $h_{\mu\nu}$ are $h_{00} = h_{11} = h_{22} = h_{33} = 2\Phi/c^2$ and $h_{0i} = A_i/c$. It should be remembered that raising or lowering a spatial (Roman) index introduces a minus sign with our adopted metric signature. Thus the numerical value of A_i is minus that of A^i , the latter being the i th component of the spatial vector \mathbf{A} . It is also worth noting that both Φ/c^2 and A_i/c are dimensionless, thereby yielding dimensionless components $h_{\mu\nu}$, which is consistent with our choice of coordinates $x^\mu = (ct, x^i)$ having dimensions of length.

¹ We adopt the following sign conventions: $(+, -, -, -)$ metric signature, $R^\rho_{\sigma\mu\nu} = 2(\partial_{[\mu}\Gamma^\rho_{|\sigma|\nu]} + \Gamma^\rho_{\lambda[\mu}\Gamma^\lambda_{|\sigma|\nu]})$, where the metric (Christoffel) connection $\Gamma^\rho_{\lambda\mu} = \frac{1}{2}g^{\rho\sigma}(\partial_\lambda g_{\mu\sigma} + \partial_\mu g_{\lambda\sigma} - \partial_\sigma g_{\lambda\mu})$, and $R^\rho_{\mu} = R^{\rho\sigma}_{\mu\sigma}$.

² Conventions in the literature vary up to a multiplicative constant for the definition of the gravitomagnetic vector potential A^i . These factors variously modify the analogues of the EM field equations and the Lorentz force law, with no scaling choice allowing all the GEM and EM equations to be perfectly analogous. Here, we follow the convention used in [29].

With the above identifications, the linearised field equations (1) with energy-momentum tensor (2) may be written in the scalar/vector form

$$\nabla^2 \Phi = 4\pi G\rho, \quad \nabla^2 \mathbf{A} = \frac{16\pi G}{c^2} \mathbf{j}, \quad (4)$$

where we have defined the momentum density (or matter current density) $\mathbf{j} \equiv \rho \mathbf{u}$, and the Lorenz gauge condition $\partial_\rho \bar{h}^{\mu\rho} = 0$ itself becomes $\nabla \cdot \mathbf{A} = 0$. Clearly, the first equation in (4) recovers the Poisson equation for the gravitational potential, familiar from Newtonian gravity, whereas the second equation determines the gravitomagnetic vector potential that describes the ‘extra’ (weak) gravitational field predicted in linearised GR, which is produced by the motion of the fluid elements in a stationary, non-relativistic source. Indeed, the general solutions to the equations (4) are given immediately by

$$\Phi(\mathbf{x}) = -G \int \frac{\rho(\mathbf{x}')}{|\mathbf{x} - \mathbf{x}'|} d^3 \mathbf{x}', \quad (5a)$$

$$\mathbf{A}(\mathbf{x}) = -\frac{4G}{c^2} \int \frac{\mathbf{j}(\mathbf{x}')}{|\mathbf{x} - \mathbf{x}'|} d^3 \mathbf{x}'. \quad (5b)$$

One may take the analogy between linearised GR and EM further by defining the gravitoelectric and gravitomagnetic fields $\mathbf{E} = -\nabla\Phi$ and $\mathbf{B} = \nabla \times \mathbf{A}$, which are easily found to satisfy the gravitational Maxwell equations

$$\begin{aligned} \nabla \cdot \mathbf{E} &= -4\pi G\rho, & \nabla \cdot \mathbf{B} &= 0, \\ \nabla \times \mathbf{E} &= \mathbf{0}, & \nabla \times \mathbf{B} &= -\frac{16\pi G}{c^2} \mathbf{j}. \end{aligned} \quad (6)$$

The gravitoelectric field \mathbf{E} describes the standard (Newtonian) gravitational field produced by a static matter distribution, whereas the gravitomagnetic field \mathbf{B} is the ‘extra’ gravitational field produced by moving fluid elements in the stationary, non-relativistic source.

The equation of motion for a test particle in the presence of the GEM fields is merely the geodesic equation (3) for the metric $g_{\mu\nu} = \eta_{\mu\nu} + h_{\mu\nu}$, from which one may determine the trajectories of either massive particles, irrespective of their speed, or massless particles, by considering timelike or null geodesics, respectively. We will assume here, however, that the test particle is massive and slowly-moving, i.e. its coordinate 3-speed v is sufficiently small that we may neglect terms in v^2/c^2 and higher. Hence we may take $\gamma_v = (1 - v^2/c^2)^{-1/2} \approx 1$, so that the 4-velocity of the particle may be written $v^\mu = \gamma_v(c, \mathbf{v}) \approx (c, \mathbf{v})$. This immediately implies that $\ddot{x}^0 = 0$ and, moreover, that $dt/d\tau = 1$, so one may consider only the spatial components of (3) and replace dots with derivatives with respect to t . Expanding the summation in (3) into terms containing, respectively, two time components, one time and one spatial component, and two spatial components, neglecting the purely spatial terms since their ratio with respect to the purely temporal term is of order v^2/c^2 , expanding the connection coefficients to first-order in $h_{\mu\nu}$ and remembering that for a stationary field $\partial_0 h_{\mu\nu} = 0$ and that one inherits a minus sign on raising or lower a spatial (Roman) index, one finally obtains the gravitational Lorentz force law

$$\frac{d\mathbf{v}}{dt} = -\nabla\Phi + \mathbf{v} \times (\nabla \times \mathbf{A}) = \mathbf{E} + \mathbf{v} \times \mathbf{B}. \quad (7)$$

The first term on the right-hand side gives the standard Newtonian result for the motion of a test particle in the field of a static, non-relativistic source, whereas the second term gives the ‘extra’ force felt by a moving test particle in the presence of the ‘extra’ field produced by moving fluid elements in the stationary, non-relativistic source.

IV. GRAVITOELECTROMAGNETIC MODELLING OF GALAXY ROTATION CURVES

The GEM formalism is applied to the modelling of galaxy rotation curves in [20], where the galactic density and velocity distribution is assumed to act as a stationary, non-relativistic matter source. Thus, somewhat unusually, the fluid pressure is assumed to vanish and the galaxy is instead modelled as consisting of a ‘dust’ of stars. This approach therefore uses the field equations (4) and the equation of motion (7), where the velocity distribution \mathbf{u} of the galaxy in the former is identified with the velocity \mathbf{v} of test particles in the latter, thereby leading to a potentially self-consistent pressureless model.

The central result in [20] can be derived straightforwardly as follows. First, one adopts cylindrical polar coordinates (R, ϕ, z) and assumes azimuthal symmetry, such that $\rho = \rho(R, z)$ and $\mathbf{v} = v(R, z)\hat{\phi}$, which from (5) implies that $\Phi = \Phi(R, z)$ and $\mathbf{A} = A(R, z)\hat{\phi}$. In this case,

$$\nabla \times \mathbf{A} = \frac{1}{R} \left(-\frac{\partial\psi}{\partial z} \hat{\mathbf{R}} + \frac{\partial\psi}{\partial R} \hat{\mathbf{z}} \right), \quad (8a)$$

$$\mathbf{v} \times (\nabla \times \mathbf{A}) = \frac{v}{R} \left(\frac{\partial\psi}{\partial R} \hat{\mathbf{R}} + \frac{\partial\psi}{\partial z} \hat{\mathbf{z}} \right), \quad (8b)$$

where we have defined the poloidal gravitomagnetic flux $\psi \equiv RA$. Also, in light of the Lorenz (or Coulomb) gauge condition $\nabla \cdot \mathbf{A} = 0$ (which is easily confirmed by direct calculation), one has

$$\nabla^2 \mathbf{A} = -\nabla \times (\nabla \times \mathbf{A}) = \left[\frac{\partial}{\partial R} \left(\frac{1}{R} \frac{\partial\psi}{\partial R} \right) + \frac{1}{R} \frac{\partial^2\psi}{\partial z^2} \right] \hat{\phi}. \quad (9)$$

The field equations (4) and the radial and vertical components of the fluid equation of motion (7) may therefore be written as

$$\frac{1}{R} \frac{\partial}{\partial R} \left(R \frac{\partial\Phi}{\partial R} \right) + \frac{\partial^2\Phi}{\partial z^2} = 4\pi G\rho, \quad (10a)$$

$$\frac{\partial}{\partial R} \left(\frac{1}{R} \frac{\partial\psi}{\partial R} \right) + \frac{1}{R} \frac{\partial^2\psi}{\partial z^2} = \frac{16\pi G}{c^2} \rho v, \quad (10b)$$

$$\frac{\partial\Phi}{\partial R} - \frac{v}{R} \frac{\partial\psi}{\partial R} = \frac{v^2}{R}, \quad (10c)$$

$$-\frac{\partial\Phi}{\partial z} + \frac{v}{R} \frac{\partial\psi}{\partial z} = 0. \quad (10d)$$

Using (10c) and (10d) to eliminate $\partial\psi/\partial R$ and $\partial\psi/\partial z$ from (10b), then using (10a) to eliminate the resulting term containing $\partial^2\Phi/\partial z^2$, the field equation (10b) yields

$$\begin{aligned} \left(v + R \frac{\partial v}{\partial R} \right) \frac{\partial\Phi}{\partial R} + R \frac{\partial v}{\partial z} \frac{\partial\Phi}{\partial z} = \\ \frac{v}{R} \left[v \left(v - R \frac{\partial v}{\partial R} \right) + 4\pi G\rho R^2 \left(1 - \frac{4v^2}{c^2} \right) \right]. \end{aligned} \quad (11)$$

The non-linear first-order partial differential equation (11) for the galactic velocity field $v(R, z)$ is the key expression in [20]³, and depends only on the galactic density distribution ρ and on the derivatives $\partial\Phi/\partial R$ and $\partial\Phi/\partial z$ of the Newtonian gravitational potential, which are themselves also determined by specifying ρ . Indeed, Φ is given by (5a), which in cylindrical

polar coordinates with azimuthal symmetry reads⁴

$$\begin{aligned}\Phi(R, z) &= -G \int_0^\infty dR' \int_0^{2\pi} d\phi' \int_{-\infty}^\infty dz' \frac{R' \rho(R', z')}{|\mathbf{x} - \mathbf{x}'|} \\ &= -2G \int_0^\infty dR' \int_{-\infty}^\infty dz' \rho(R', z') R' \sqrt{\frac{m}{RR'}} K(m),\end{aligned}\quad (12)$$

where $K(m)$ is a complete elliptic integral function of the first kind and $m = 4RR'/[(R + R')^2 + (z - z')^2]$. Moreover, the derivatives $\partial\Phi/\partial R$ and $\partial\Phi/\partial z$ may also be expressed analytically as

$$\frac{\partial\Phi}{\partial R} = G \int_0^\infty dR' \int_{-\infty}^\infty dz' \rho(R', z') \frac{R'}{R} \sqrt{\frac{m}{RR'}} \left[K(m) + \frac{1}{2} \left(\frac{R}{R'} - \frac{2-m}{m} \right) \frac{mE(m)}{1-m} \right], \quad (13a)$$

$$\frac{\partial\Phi}{\partial z} = \frac{G}{2} \int_0^\infty dR' \int_{-\infty}^\infty dz' \rho(R', z') \left(\frac{z - z'}{R} \right) \sqrt{\frac{m}{RR'}} \frac{mE(m)}{1-m}, \quad (13b)$$

where $E(m)$ denotes a complete elliptic integral of the second kind.

Before considering further the application of equation (11) to modelling galaxy rotation curves, we note that, if one neglects the mass currents on the RHS of (10b) (by letting $c \rightarrow \infty$), then one may consistently set $\psi = 0$ (although other solutions to the resulting homogeneous equation (10b) do exist). The radial and vertical components of the fluid equation of motion (10c)–(10d) then immediately yield $\partial\Phi/\partial z = 0$ and thus $v^2(R) = R\partial\Phi/\partial R$, where the latter is the usual Newtonian equation assumed in the modelling of galaxy rotation curves.

In applying the full equation (11) to the modelling of galaxy rotation curves, it is noted in [20] that observations of the rotation velocity are typically made along the galactic equatorial plane, so one may take $z = 0$. Assuming further a galactic density distribution that is symmetric about this mid-plane, (11) then reduces to

$$\begin{aligned}\left(\beta + R \frac{\partial\beta}{\partial R} \right) \frac{\partial\Phi(R, 0)}{\partial R} &= \\ \frac{c^2\beta}{R} \left[\beta \left(\beta - R \frac{\partial\beta}{\partial R} \right) + \frac{4\pi G}{c^2} \rho(R, 0) R^2 (1 - 4\beta^2) \right],\end{aligned}\quad (14)$$

where we have defined $\beta(R) \equiv v(R, 0)/c$. Equation (14) is applied in [20] to two different models of the galactic density distribution.

The first model considered uses the density and gravitational potential given by the analytical Miyamoto–Nagai (MN) solution to Poisson's equation [30]. In this approach, one begins

by assuming the fairly simple potential form

$$\Phi(R, z) = -\frac{GM}{\sqrt{R^2 + (a + \sqrt{b^2 + z^2})^2}}, \quad (15)$$

where M is the total galactic mass and a and b are free positive parameters. The density distribution implied by Poisson's equation is then given by

$$\begin{aligned}\rho(R, z) &= \\ \frac{Mb^2}{4\pi} \times \frac{aR^2 + (a + 3\sqrt{b^2 + z^2})(a + \sqrt{b^2 + z^2})^2}{\left[R^2 + (a + \sqrt{b^2 + z^2})^2 \right]^{5/2} (b^2 + z^2)^{3/2}},\end{aligned}\quad (16)$$

which extends to infinity in both R and z . The constant density contours have the form of spheroids of revolution with semi-axes proportional to a and b . It is straightforward to verify that, when integrated over all space, this density distribution yields the total mass M . In [20], this model is fitted to the observed rising rotation curve of NGC 1560 out to 8.3 kpc by varying the parameters M , a and b . The derived parameter values are $M = 7.3 \times 10^{10} M_\odot$, $a = 0.373$ kpc and $b = 0.300$ kpc, which yield a reasonable fit to the rotation curve, but does not reproduce the luminosity profile of NGC 1560. This occurs because the infinite spheroidal solution does not describe the equilibrium of a finite disk-like object, and thus fails to reproduce its mass distribution and total mass.

Consequently, in the second model, the galaxy is instead considered as an axisymmetric thin disk of finite radius, which is again symmetric about its mid-plane $z = 0$. The density distribution is assumed to have the functional form

$$\rho(R, z) = \rho(R, 0) \exp\left(-\frac{z^2}{2\Delta^2(R)}\right), \quad (17)$$

where $\Delta(R)$ is a characteristic disk width with some assumed radial dependence. For small values of $\Delta(R)$, one can estimate

³ Equation (11) does, in fact, differ slightly from equation (4.1) in [20], since the latter lacks the factor of 4 multiplying v^2/c^2 in the final term on the RHS. We believe the expression in [20] to be in error as a consequence of the choice of scaling used in the definition therein of the gravitomagnetic vector potential \mathbf{A} .

⁴ Our final expression for Φ differs by a factor of 2 as compared to equation (4.2) in [1]; we believe the latter to be in error.

the integral over z' in (13a) analytically using the Laplace approximation, which boils down to setting $z' = 0$ in the integrand and multiplying by the volume $\sqrt{2\pi}\Delta(R)$ of the Gaus-

sian factor in (17); this yields

$$\frac{\partial\Phi(R,0)}{\partial R} \approx 2\sqrt{2\pi}G \int_0^\infty \frac{R'\rho(R',0)\Delta(R')}{R(R+R')} \left[K\left(\frac{4RR'}{(R+R')^2}\right) + \frac{R+R'}{R-R'} E\left(\frac{4RR'}{(R+R')^2}\right) \right] dR'. \quad (18)$$

To evaluate the above integral (numerically), the density distribution $\rho(R,0)$ is taken from the luminosity profile of the galaxy under consideration, which is therefore reproduced *automatically*, but one still requires a model for the radially-dependent characteristic vertical width $\Delta(R)$ of the galaxy. In [20], this is taken to coincide with a given constant density contour of the analytical MN solution (16). In particular, one defines $\Delta(R)$ such that

$$\frac{\rho_{MN}(R, \Delta(R))}{\rho_{MN}(0,0)} \frac{\mathcal{M}(\ell)}{M} = \exp\left(-\frac{\ell^2}{2}\right), \quad (19)$$

where $\rho_{MN}(R, z)$ denotes the right-hand side of (16), ℓ is a pre-defined ‘label’, which is usually set to $\ell = 3$ so that the chosen contour contains a fraction (approximated by $1 - \exp(-\ell^2/2) = 0.989$) of the total mass M , and $\mathcal{M}(\ell)$ is the resulting approximate mass of the galaxy with the density distribution (17), estimated by using the Laplace approximation to perform the integral over z :

$$\mathcal{M}(\ell) = (2\pi)^{3/2} \int_0^{R_{\max}} \Delta(R') \rho(R',0) R' dR', \quad (20)$$

where the maximum radius of the galactic disk, R_{\max} , is obtained by solving (19) with $\Delta(R) = 0$. This approach requires quite a time-consuming iterative process, but the velocity profile again depends only on the three free parameters M , a and b . When fitted to the same observed rising rotation curve data for NGC 1560 as used above, the derived parameter values for this model are $M = 1.52 \times 10^{10} M_\odot$, $a = 7.19$ kpc and $b = 0.567$ kpc (yielding $R_{\max} = 12.2$ kpc), which again produces a reasonable fit to the rotation curve, but now also reproduces the luminosity profile of NGC 1560 by construction. The model is also used in [20] to reproduce satisfactorily the observed rotation curve data for the spiral galaxy NGC 3198 and the lenticular galaxy NGC 3115.

V. PROBLEMS WITH THE MODEL

Although the approach outlined above appears at first sight to be a reasonable methodology for modelling galaxy rotation curves using the GEM formalism, it does have some unusual features. As mentioned previously, the model most notably assumes that the galaxy consists of a pressureless ‘dust’ of stars, all of which follow circular orbits. In particular, this means that the vertical support necessary to maintain dynamical equilibrium is assumed all to arise from gravitomagnetic

rotational effects, which we will see leads to such effects being massively overestimated. This shortcoming may be addressed by, for example, using a distribution function approach based on the GEM formulation of the Jeans equation [28], since this enables vertical support via a velocity dispersion of the stars, and also allows for individual stars to follow non-circular orbits whilst retaining net currents that are strictly azimuthal.

Whilst the more sophisticated approach of distribution functions makes better physical sense, we will not concern ourselves with such modifications here, since we wish merely to address why the methodology outlined in Section IV can lead to incorrect conclusions regarding the effect of gravitomagnetism on galactic rotation curves. Indeed, we will limit our considerations still further by choosing not to pursue the iterative numerical process for obtaining rotation curves for the thin disk density model (17), since this is rather computationally cumbersome and time consuming. Instead, we will restrict our attention here to the model having the MN density profile (16), which can be treated almost entirely analytically and suffices to demonstrate the shortcomings of the overall approach outlined in Section IV.

A. Order of magnitude analysis

Before considering the single key equation (11) that forms the basis of the approach outlined in Section IV, we begin by making some observations regarding the four separate equations (10) from which (11) is derived. In particular, we first note that in the radial equation of motion (10c) one requires a term in v^2 to obtain sensible results. This occurs because v is $\mathcal{O}(\sqrt{\Phi})$ rather than $\mathcal{O}(\Phi)$. Indeed, one can see from the set of equations (10) that in typical circumstances there will exist a hierarchy of magnitudes for different quantities, and it is worth describing this hierarchy now so as to orient ourselves.

This is most easily achieved by first adopting geometric units $G = c = 1$, which we will assume henceforth. One then requires only a single scale to specify the base of units, which in this application is most conveniently taken to be length. In particular, we take the unit of length to be 1 kpc, which corresponds to typical galactic scales. All other physical quantities can then be expressed in terms of this base unit. For example, a mass M in SI units is given in terms of our units by $GM/c^2 \times 1 \text{ kpc m}^{-1}$, whereas a density ρ in SI units is given by $G\rho/c^2 \times 1 \text{ kpc}^2 \text{ m}^{-2} \approx 7.07 \times 10^{11} \rho$. Thus, typical galactic densities of $\sim 2 \times 10^{-19} \text{ kg m}^{-3}$ correspond to $\sim 1.4 \times 10^{-7}$

in our units. For a broad selection of galaxies types, one may therefore take typical densities in our units to lie in the range $\mathcal{O}(10^{-8})$ to $\mathcal{O}(10^{-6})$; we will take the upper of these as indicative, since this maximises the magnitude of gravitomagnetic effects, although in reality they will usually be somewhat smaller.

From the Poisson equation (10a), or its more succinct form in (4), one sees that $|\Phi|$ is also $\mathcal{O}(10^{-6})$, and hence the velocity $v \sim \mathcal{O}(10^{-3})$ (where to convert velocities in SI unit to our units, one needs merely to divide by c). Then, from equation (10b), which one can also write more usefully as $\nabla^2\psi = 16\pi R\rho v - (2/R)\partial\psi/\partial R$, one sees that $|\psi| \sim \mathcal{O}(10^{-9})$, modulo any multiplicative effects from R which are limited to a factor of ~ 10 for a typical galaxy.

Now considering either the radial equation of motion (10c) or its vertical counterpart (10d), one sees any effects arising from ψ , which always appears multiplied by v , must be $\mathcal{O}(10^{-6})$ *smaller* than those arising from Φ . Consequently, any gravitomagnetic effects will have a negligible effect on the circular velocity of a test particle, which will very well approximated simply by the strictly Newtonian expression $\sqrt{R\partial\Phi/\partial R}$.

This result is at least allowable (notwithstanding the usual clash, if no dark matter is assumed, with the flat or rising rotation curves observed in many galaxies), if disappointing, but one sees from the vertical equation of motion (10d) that there is a much more serious problem. In this case, one requires the $\mathcal{O}(10^{-6})$ term in Φ to be balanced by the $\mathcal{O}(10^{-12})$ term in ψ ; this is simply impossible and indicates that the set of

equations (10) has no physically meaningful solution. As mentioned above, this problem arises because one has insisted that all the vertical support force arises from gravitomagnetic effects, which is impossible for ordinary matter.

B. Rotation curves for the MN density profile

In eliminating various quantities between the equations (10) to arrive at the ‘master’ equation (11) in [20], one can no longer identify the issues discussed above. Indeed, one can go on to find solutions ψ that satisfy (11), although these cannot be physically meaningful, as our analysis above shows. We now illustrate this directly by considering a galaxy having the MN density profile (16) and gravitational potential (15), which was the first model used in [20] to fit the observed rotation curve data of NGC 1560 (although it fails to reproduce its luminosity profile). As discussed above, the resulting derived parameters are $M = 7.3 \times 10^{10} M_\odot$, $a = 0.373$ kpc and $b = 0.300$ kpc, so the fitted MN density profile is moderately oblate. The resulting gravitational potential and density contours are shown in Figure 1.

Inserting the forms for the MN potential (15) and density (16) into the ‘master’ equation (11) yields a very complicated expression, but one can make progress analytically if one restricts attention to the equatorial plane $z = 0$, as in (14). This is permissible since, although (11) contains the z -derivative of the potential Φ , one can see that for the MN form of the potential this vanishes on the equatorial plane. The resulting equation then reads $A + B = 0$, with

$$A = -R^2 M \left[-bR (R^2 + a^2 + 2ba + b^2) \frac{dv}{dR} + (2b^3 + 5b^2a + (4a^2 - R^2)b + R^2a + a^3) v \right] \quad (21a)$$

$$B = 4 \left[\frac{1}{4} b (R^2 + a^2 + 2ba + b^2)^{5/2} \left(\frac{dv}{dR} R - v \right) + MR^2 v (5a^2b + a^3 + R^2a + 3b^3 + 7b^2a) \right] v^2, \quad (21b)$$

where we have split the LHS into the terms, since it is possible to obtain a simple analytic result for v by just setting $A = 0$. It is not immediately obvious that this is a valid procedure, even as an approximation, since $v \sim \mathcal{O}(10^{-3})$ and ρ , and by extension its volume integral M , are likely $\mathcal{O}(10^{-6})$. Thus, both expression A and the first half of the terms in B are likely $\mathcal{O}(10^{-9})$, and hence it is not clear that one can preferentially drop the first half of B . Numerically, however, it transpires that the value of $M = 7.3 \times 10^{10} M_\odot$ derived for NGC 1560 is sufficiently large that one can consider just $A = 0$, and we note that this yields an expression for v that is in fact *independent* of M .

We may illustrate this approach explicitly by comparing the exact and approximate solutions for v in this case. Setting just $A = 0$ and solving for v gives

$$v = \frac{CR^{2+\frac{a}{b}}}{[R^2 + (a+b)^2]^{3/2}}, \quad (22)$$

where C is an arbitrary constant. In Figure 2, we show the ro-

tation curve resulting from the analytical approximation (22) as the red curve and an exact numerical integration of the full equation (21) as the black curve. For the analytic approximation, although there is no dependence on mass, one must provide an overall scaling C , and a value of $C = 1/6400$ was used in the plot, which gives reasonably good agreement between the exact result in this case. The latter was calculated by numerical integration starting at the outermost rotation curve data point for NGC 1560, for which $v = 2.67 \times 10^{-4}$ (in units of c) at $R = 8.29$ kpc, and moving inwards towards the origin, in the same way as performed in [20]. Similarly, one could instead fix the scaling C of the analytical result by ensuring that it passes through the outermost data point, which moves the red curve up slightly.

In any case, it is important to note that, while the fit to the NGC 1560 rotation curve data in [20] yields the derived mass $M = 7.3 \times 10^{10} M_\odot$, the only information about M is in quite small changes in the *shape* of the curve that occur as M drops below this best-fit value. For *larger* values of M , the shape

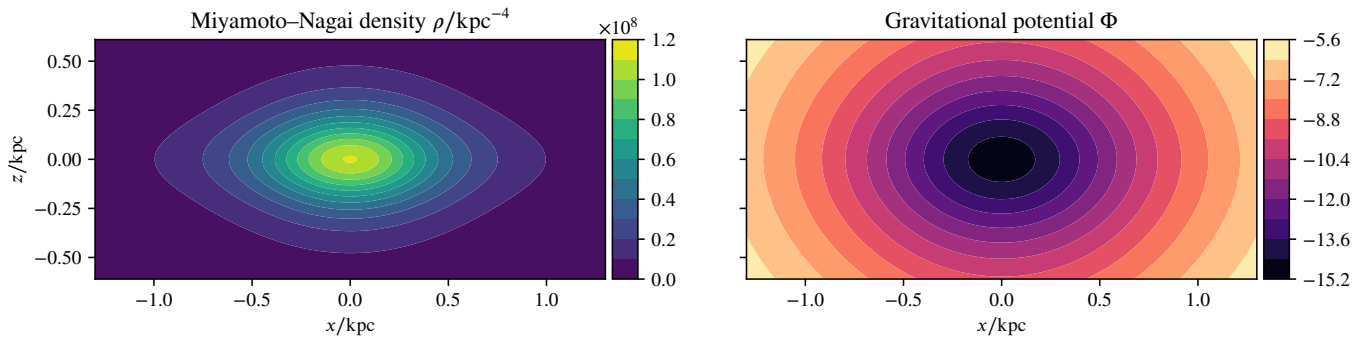


FIG. 1. Gravitational density (left) and potential (right) contours for a MN profile with parameters a and b derived from fitting the rotation curve of NGC 1560 in [20].

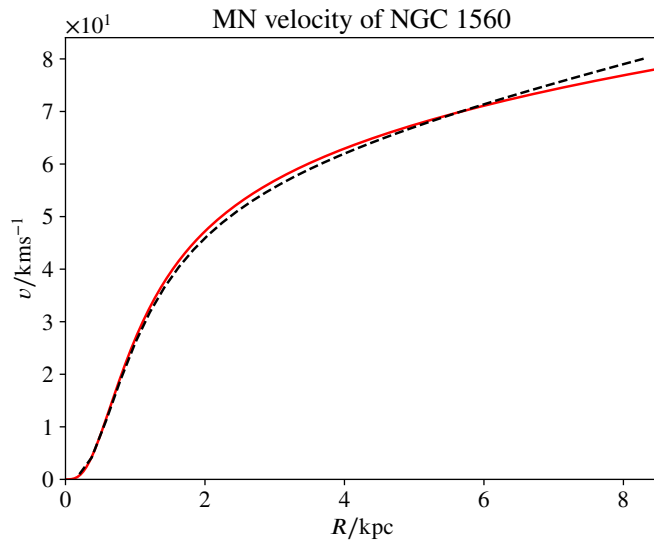


FIG. 2. Rotation velocity v (in units of c) versus R in kpc for a MN profile with parameters derived from NGC 1560. The red curve is obtained using the analytical approximation (22) with $C = 1/6400$ and the black curve is an exact numerical integration using equation (21).

of the curve is invariant, and corresponds to that given in the analytical approximation (22), which does not depend on M . This suggests that there may be a large uncertainty on the mass M derived from the rotation curve data, although no errors on the fitted value are provided in [20].

Nonetheless, let us assume the best-fit value of M to calculate also the rotation curve that one would obtain in the absence gravitomagnetic effects, i.e. $\psi = 0$, and the galaxy is completely static and supported just by usual pressure forces. In this case, the rotational velocity of a test particle is merely $\sqrt{R\partial\Phi/\partial R}$ and one obtains the red curve in Figure 3, which we plot alongside the exact rotation curve (in black) from Figure 2, which includes gravitomagnetic effects. Figure 3 matches very well with Figure 2 in [20], but is worthy of further comment. First, we note that the conventional rotation curve peaks at velocities around 420 km s^{-1} (readopting SI units for the moment); this is much higher than one would ex-

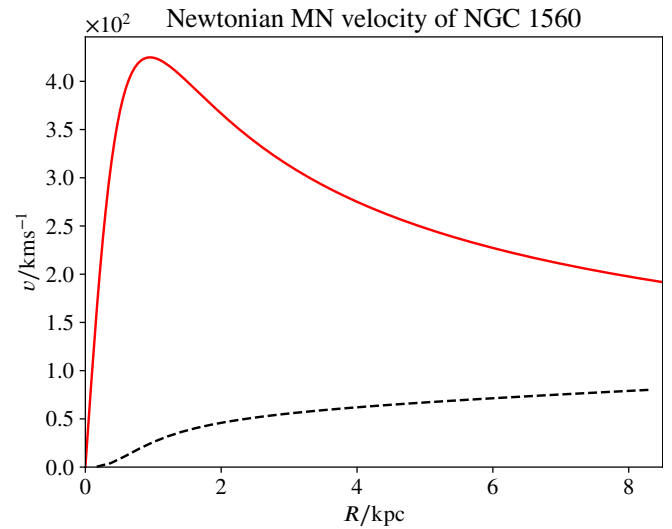


FIG. 3. The conventional Newtonian rotation curve (red) for NGC 1560 assuming a MN profile with the best-fit values of the parameters a , b and M from [20], together with the exact rotation curve including gravitomagnetic effects (black), already shown in Figure 2.

pect for what is meant to be a dwarf galaxy. Second, and more important, we see that the effects of gravitomagnetism here are to *suppress* the rotational velocity of test particles, not *enhance* them. Thus one requires a great deal more matter present in the case with gravitomagnetic effects than that without, in order to explain a given rotation curve level. Gravitomagnetic effects serve here to explain only aspects of the *shape* of rotation curves (here a gradually rising one), but absolutely not whether one requires more matter than appears visible; in other words, it makes the missing matter problem *worse*.

Before moving on to discuss the issue of gravitomagnetic vertical support (or the lack thereof) in the next subsection, it is worth noting some further aspects of the shape of the rotation curves derived above. Although the rotation curves obtained using either (21) or the analytic approximation (22) appear to fit the rotation curve data for NGC 1560 shown in Figure 1 of [20] in a pleasing way, this disguises the problem that the shape of these rotation curves changes considerably with just small changes in the a and b parameters.

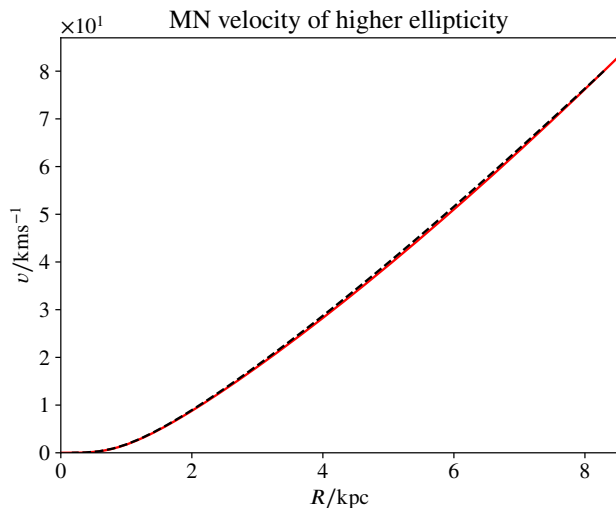


FIG. 4. Same as Figure 2, but for a higher ellipticity case, with $a = 0.7$ kpc and $b = 0.3$ kpc.

Observations of NGC 1560 in the visible show it to be considerably more ‘elliptical’ than the ratio $a : b = 0.373 : 0.300$ indicates, with a ratio of $\sim 0.7 : 0.3$ seeming much more appropriate. From the analytical expression (22), however, one can see that this will cause a problem, since the shape of the predicted rotation curve will scale as $v \propto R^{1.33}$ at large R , and so it will be concave rather than convex towards the R axis. Indeed, this will clearly occur for any ratio $a : b > 2 : 1$. No known rotation curves have this shape (concave rather than convex over their whole range), and so this model will be incapable of accommodating galaxies with ellipticities beyond this ratio. That this is not an artefact of our analytical approximation is illustrated in Figure 4, which is the equivalent of the rotation curves plot in Fig. 2, but for a and b values of 0.7 and 0.3 kpc, and using the same mass M . One sees that the red curve (analytical approximation) closely follows the black curve (exact numerical integration), and hence the insights that the analytic approximation (22) provides for what occurs at higher $a : b$ ratios are indeed borne out in the exact integration.

C. Gravitomagnetic vertical support

As our final point in this section we now discuss further the assumption that all vertical support for dynamical equilibrium is provided by gravitomagnetic rotational effects, which in our opinion is the key issue with the modelling approach outlined in Section IV, and applies irrespective of the assumed density profile of the galaxy. As above, however, we will illustrate our findings for the MN profile, since it can again be treated almost entirely analytically.

In particular, we will show that in order to provide the vertical support necessary, ψ has to become infinite at the origin, and have extremely large values near to it. To substantiate this, plus gain some insight into what is happening analytically, we again take a ‘dual track’ approach in which we carry out exact

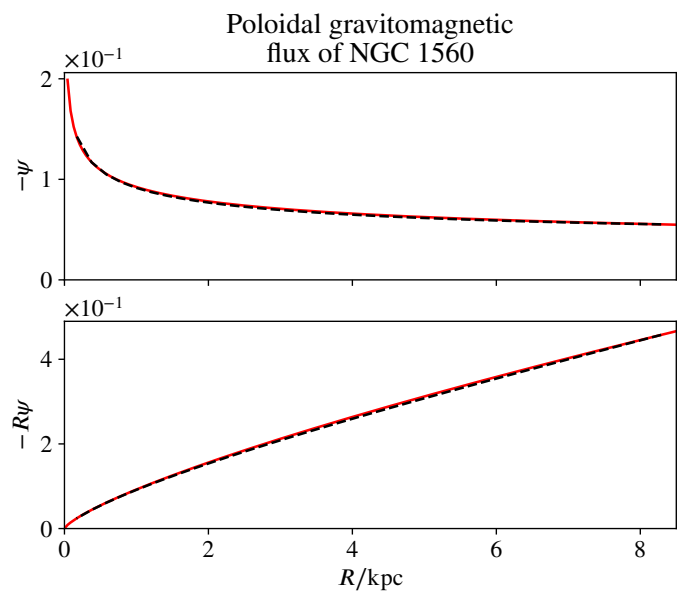


FIG. 5. Top: the function $-\psi$ versus R in kpc using the parameters derived for NGC 1560 in [20]. Bottom: the function $-R\psi$, to indicate better the behaviour near the origin. In each case the black curve is the result of an exact numerical integration, and the red curve shows the analytic approximation (23).

numerical integrations, as well as develop an analytical approximation. To this end, one can construct an exact ODE in R applicable in the equatorial plane by using radial equation of motion (10c), together with our analytical approximation for circular velocity v in (22). One can then form an approximation to ψ based on the smallness of the coefficient C , which yields the very simple approximate solution

$$\psi = \frac{MbR}{C(b-a)R^{\frac{a}{b}}}. \quad (23)$$

Using the values of the parameters derived for NGC 1560 in [20], this approximation is in fact even better than that for the rotation curve in (22), as we demonstrate in Fig. 5. The curves for the exact numerical integration (black) and the analytic approximation from (23) (red) are virtually indistinguishable. One sees that ψ itself diverges towards the origin, whereas $R\psi$ converges at the origin; this is consistent with the ratio $a/b = 0.373/0.3$ lying between 1 and 2, and hence according to (23) $R\psi$ should go to zero at $R = 0$, whereas ψ diverges.

By comparison, in Fig. 6 we show $R\psi$ for the higher ellipticity case considered above, i.e. $a/b = 0.7/0.3$. We have plotted only $R\psi$ here since even this diverges, as to be expected from (23) with $a/b > 2$. We also note that in all of these plots of ψ the values involved are $\mathcal{O}(1)$ or perhaps $\mathcal{O}(10^{-1})$, which is roughly 10^{8-9} larger than expected to be generated by GEM effects, according to the orders of magnitude analysis given earlier.

This effect must originate from the unwitting inclusion of *free-space* solutions of the Poisson-like equation (10b) that determines ψ , i.e. solutions for which the source term on the

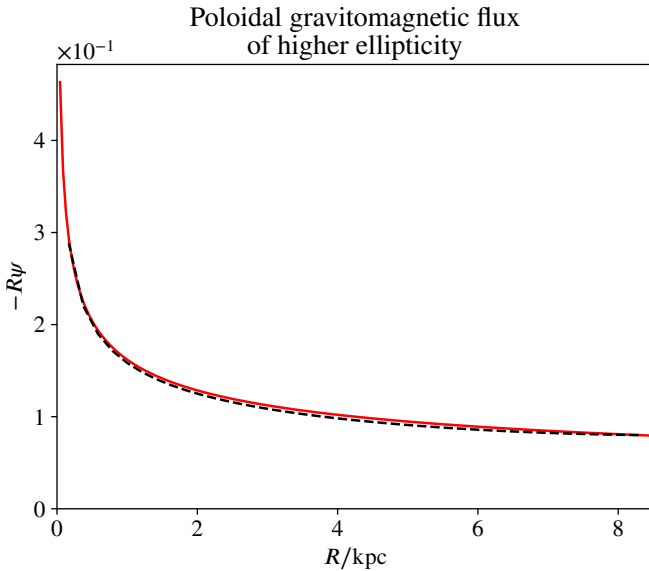


FIG. 6. Same as the Figure 5 (bottom), but for a higher ellipticity case, with $a/b = 0.7/0.3$.

RHS, which would normally generate ψ , are set to zero. One can introduce arbitrary amounts of such homogeneous solutions to any solution of the inhomogeneous equation. However, the penalty is of course that any such solution has to add in singularities at either infinity or the origin. If this were not the case, one would be free to add homogeneous solutions of arbitrary amplitude to, for example, the Poisson equation for the gravitational field around the Sun or Earth, meaning one would lose the ability to predict the force of gravity based on the mass of an object. Such a procedure is forbidden by the need to exclude singularities.

Thus, having demonstrated that a singularity exists (at the origin in this case) with the GEM approach outlined in Section IV, this should definitively rule out the methodology as a means of explaining flat galaxy rotation curves without dark matter. It might be argued that a ‘get-out’ might exist since most galaxies already contain a singularity near their centres in the form of supermassive black holes. However, such a model would require separate computations that we have not seen carried out as yet to establish it, and a priori seems contrived. Finally, although we have not gone into it here, one finds further that a singularity can exist even if ψ does not diverge, since it turns out that to have the spacetime metric obey ‘elementary flatness’ [31], one requires not only that ψ is not divergent as R approaches zero, but must behave as $\psi \propto R$ for small R . The ψ functions discussed here are far from having this property, and indeed violate this requirement all the way up the z -axis, posing a further problem for this line of approach.

VI. HOMOGENEOUS POLOIDAL SOLUTIONS

In Section VC we alluded to the unwitting inclusion in [20] of homogeneous solutions to the Poisson-like equation Eq. (10), which can seemingly facilitate large and inter-

esting departures from the Newtonian rotation formula. Even more recently in fact, an attempt has been made in [21] to capitalise directly on these solutions in an effort to bring about the same effect. In this final section, we demonstrate that the homogeneous solution approach is not viable.

A. No prospects without thin disks

We will prefer still to consider an extended, axisymmetric source, such as that of the MN density profile in Eq. (15). In contrast, the authors of [21] consider only an infinitesimal, equatorial thin disk with finite surface density. In the thin disk case, the poloidal gravitomagnetic flux $\psi = \psi(R, z)$ may be completely described by a Hankel-transformed function $\tilde{\psi} = \tilde{\psi}(\lambda, z)$, where

$$\psi(R, z) = \int_0^\infty d\lambda' R e^{-\lambda'|z|} \tilde{\psi}(\lambda') J_1(\lambda' R). \quad (24)$$

If (24) holds as presented in [21] (and we will find in Section VI B that it does not), then in the case of an extended density profile the linearity of the vector Poisson equation Eq. (5) implies that the poloidal flux at a point may be associated with a distribution of thin disks

$$\psi(R, z) = \int_0^\infty d\lambda' R \tilde{\Psi}(\lambda', z) J_1(\lambda' R), \quad (25a)$$

$$\tilde{\Psi}(\lambda, z) \equiv \int_{-\infty}^\infty dz' e^{-\lambda|z-z'|} \tilde{\psi}(\lambda, z'). \quad (25b)$$

By substituting Eq. (25a) into Eq. (10) and taking an inverse Hankel transform we then find

$$\frac{1}{\lambda} \frac{\partial \tilde{\Psi}(\lambda, z)}{\partial z} = \int_0^\infty dR' \frac{R'}{v(R', z)} \times \frac{\partial \Phi(R', z)}{\partial z} J_1(\lambda R'), \quad (26)$$

while applying the same steps to Eq. (10), in combination with the recurrence relation for Bessel functions, yields

$$\tilde{\Psi}(\lambda, z) = \int_0^\infty dR' \left[v(R', z) + \frac{R'}{v(R', z)} \frac{\partial \Phi(R', z)}{\partial R'} \right] J_0(\lambda R'). \quad (27)$$

In the (anyway unphysical) limit of a thin disk, inspection of Eq. (24) suggests we may be justified in using the relation

$$\frac{\partial \tilde{\Psi}(\lambda, z)}{\partial z} \rightarrow -\text{sgn}(z) \lambda \tilde{\Psi}(\lambda, z). \quad (28)$$

Precisely Eq. (28) is used in [21] to relate the integrals in Eqs. (26) and (27), and this is done effectively in the singular environment of the disk itself, at $z = 0$. Given this relation of integrals, the authors then take the curious step of equating the

integrands, arriving at an apparently deterministic expression for the rotational velocity at all radii

$$v(R', 0)^2 = -R' \frac{\partial \Phi(R', 0)}{\partial R'} - \frac{R' J_1(\lambda R')}{J_0(\lambda R')} \left(\frac{\partial \Phi(R', z)}{\partial z} \right)_{z=0}. \quad (29)$$

In Eq. (29) we retain the prime on R' to remind ourselves that a dummy variable has somehow ended up on the *outside* of a putatively physical equation. In Eq. (29) the second term on the right hand side constitutes a correction to the Newtonian rotation curve. This correction looks appealing because it is also sourced by the gravitational potential in a strict manner: the axial gravitoelectric field strength close in to the singular plane will approach the surface density of matter in the thin disk, according to the Gaussian ‘pill-box’ construction. This correction is tunable by a ratio of Bessel functions, in which the conjugate Hankel radius appears as a single free parameter. By tuning this parameter, the poles introduced by the Bessel coefficient can be driven off to some distant extragalactic scale. The *intragalactic* rotation curve on the other hand, which then looks as though it is being computed deterministically from the surface density profile, may indeed depart from the Newtonian and become flat or rising.

Whether or not Eq. (29) has any physical meaning, we can at least conclude that the mathematical steps which produced it cannot be replicated without Eq. (28), i.e. the construction of [21] *requires* a singular disk. In the physical case of an extended profile, Eqs. (26) and (27) can only be related by differentiating under the integral sign of Eq. (27). If we then repeat the remarkable step of equating the integrands, the closest we can get to Eq. (29) is the following

$$\frac{\lambda R' J_1(\lambda R')}{v(R', z) J_0(\lambda R')} \frac{\partial \Phi(R', z)}{\partial z} = \frac{\partial}{\partial z} \left[v(R', z) + \frac{R'}{v(R', z)} \frac{\partial \Phi(R', z)}{\partial R'} \right]. \quad (30)$$

In common with Eq. (29), the true relation Eq. (30) contains a deterministic correction, relative the Newtonian rotational velocity prediction, which is somewhere singular and freely tuned by the conjugate Hankel radius. However the implications of the new relation are fundamentally different: at every (dummy) radius R' the velocity is determined by an ODE in the axial z direction. This ODE requires some initial data for each (dummy) R' , which might as well be provided by some *user-defined* rotation curve $v(R', 0)$ in the (dummy) equatorial plane. Thus, Eq. (30) requires the equatorial rotation curve as an input, and does not supply it as an output.

If some initial data $v(R', 0)$ is chosen, Eq. (30) can propagate the rotational velocity axially above and below the equatorial plane, depending strictly on the gravitoelectric potential $\Phi(R', z)$ and the tunable Hankel radius λ . Because Eq. (30) modifies the axial derivative of the Newtonian expression, we can still depart from the Newtonian rotational velocity above

and below the equatorial plane even if we use the Newtonian expression for $v(R', 0)$. This is illustrated in Fig. 7, where the MN profile associated with NGC 1560 is used to propagate Eq. (30) using precisely the Newtonian rotational velocity of that profile as initial data. With other initial data, doubtless even more interesting effects may be produced by Eq. (30): there are apparently as many possibilities as there are functions on the positive real line, and this is not the kind of situation we expect to encounter in a well posed theory of gravity such as GR. We will now clarify in Section VI B why the construction underpinning [21] and our corollary in Eq. (30) do not — and can never — arise in nature.

B. No prospects without sources

The authors of [21] attempt to make a distinction between what happens in determining the potential from the matter density distribution, and how the poloidal gravitomagnetic field is determined (or not) by the matter flows. In particular for the first case (density) they correctly say that our equation Eq. (10) ‘completely fixes the value of the Newtonian potential everywhere’, whereas for the poloidal gravitomagnetic field ψ in Eq. (24), there is meant to be a freedom in adding in homogeneous solutions of the equation which determines it. Since we do not agree with this distinction, we will start with the case of how the potential is uniquely determined by ρ and then show how exactly the same procedure applied to ψ again leads to unique solutions, to which we cannot add in extra homogeneous components. Despite these problems, the Hankel transform approach used by [21] is useful since it enables us to explicitly find the homogeneous solutions in question explicitly, and thereby show they are inadmissible.

In order to make sure that we do not introduce unnecessary singularities, we will work not with the ‘thin disk’ approximation used by [21], but continue from Section VI A with a continuous and differentiable distribution of matter, which we can call a thick disk. The MN profile used earlier would be a good example of what we have in mind here. After obtaining the results we will look at the thin disk limit, and show — unlike in the previous analysis in Section VI A — that it behaves in exactly the same way as found here for the thick disk. We take this as an indicator that we are finally connecting with the correct physics, and that our results are equally applicable to the case treated in [21].

We thus start with the equivalent of Eq. (25a), but for potential rather than the poloidal field, and write

$$-\Phi(R, z) = \int_0^\infty f(\lambda', z) J_0(\lambda' R) \lambda d\lambda'. \quad (31)$$

The function $f(\lambda, z)$ is thus the Hankel transform, in the R direction, of minus the potential.

Note particularly that, contrary to what is done in Eq. (25b), at this stage we are *not* going to assume a particular form for $f(R, \lambda)$. This is because we will be able to *deduce* the equivalent form for f from the equations themselves, which is an interesting feature of the approach here.

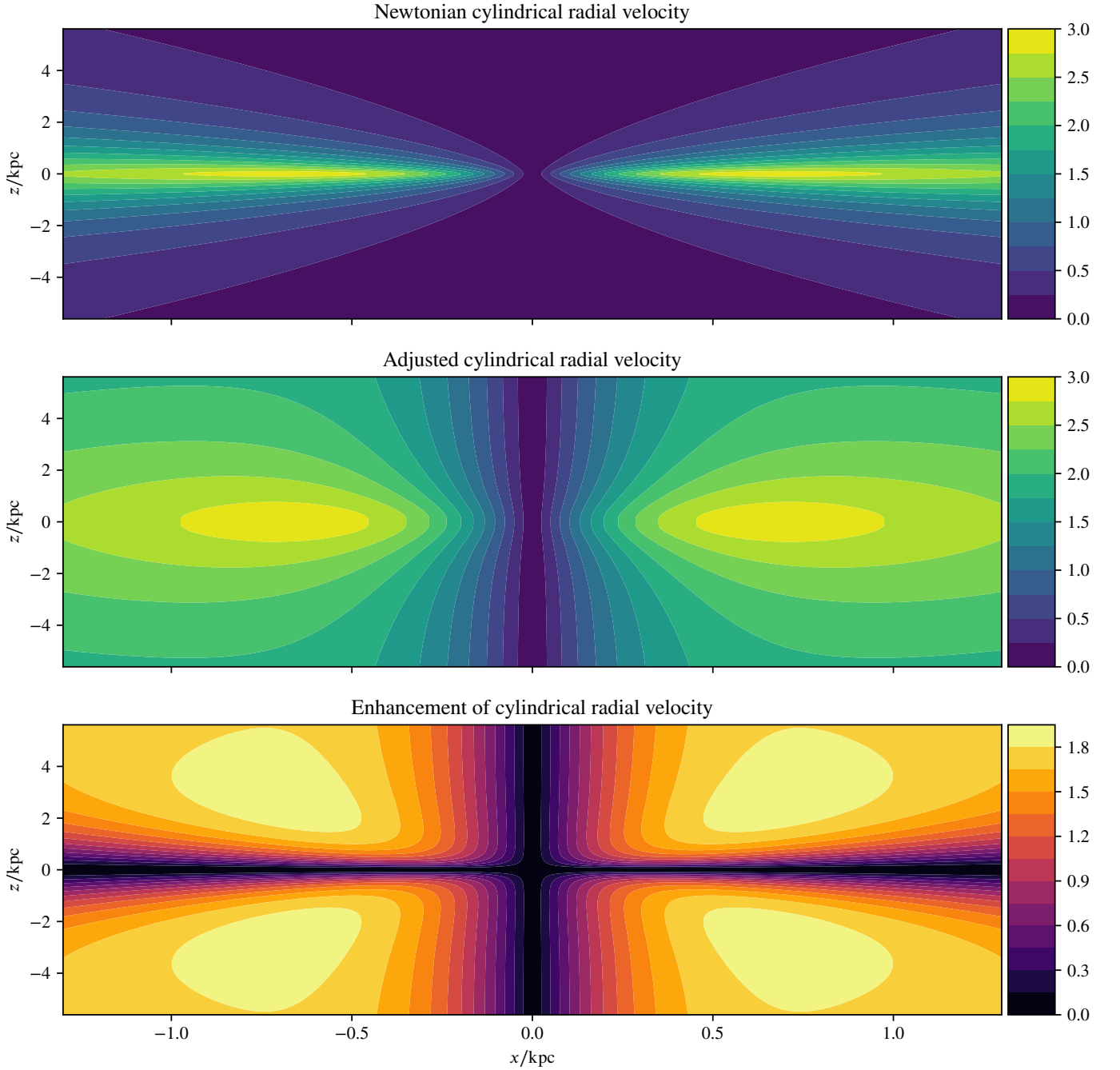


FIG. 7. Non-equatorial enhancement of the rotational velocity of the MN profile obtained by generalising the approach of [21] to extended sources. The Newtonian velocity is shown in the top frame for the MN potential in Eq. (15), as plotted in Fig. 1 for parameters associated with NGC 1560 in [20]. The middle frame shows the enhancement in the case where the equatorial rotational velocity (initial data) is identical to the Newtonian, and Eq. (30) allows this to be propagated axially using the potential. In the lower frame, the difference between enhanced and Newtonian velocities is shown, indicating a substantial velocity increase in annular zones above and below the galactic plane. The inverse Hankel radius in this case is $\lambda = 1 \times 10^{-10} \text{ kpc}^{-1}$, so that the pole introduced by the first zero of the Bessel function is expelled from the observable Universe. We show that these effects result from the misuse of homogeneous solutions for the poloidal gravitomagnetic flux.

We now insert (31) into the Poisson equation for Φ , obtaining

$$\int_0^\infty \left(\frac{\partial^2 f}{\partial z^2} - \lambda'^2 f \right) J_0(\lambda' R) \lambda' d\lambda' = -4\pi\rho(R, z). \quad (32)$$

Taking the inverse Hankel transform of each side then yields

$$\frac{\partial^2 f}{\partial z^2} - \lambda^2 f = -4\pi \int_0^\infty \rho(R', z) J_0(\lambda R') R' dR'. \quad (33)$$

This is a linear equation for f which we can solve by the

method of *variation of parameters*. In this technique, if we know solutions of the homogeneous equation for f we can use them in constructing solutions of the inhomogeneous equation via integrations involving their product with the inhomogeneous part of the equation. In the current case this yields the following full solution for f :

$$f(\lambda, z) = F_1(\lambda)e^{-\lambda z} + F_2(\lambda)e^{\lambda z} - \frac{2\pi}{\lambda} \left(e^{\lambda z} \int_a^z e^{-\lambda z'} \tilde{\rho}(\lambda, z') dz' - e^{-\lambda z} \int_b^z e^{\lambda z'} \tilde{\rho}(\lambda, z') dz' \right). \quad (34)$$

In this equation $\tilde{\rho}(\lambda, z)$ is the Hankel transform of ρ , i.e.

$$\tilde{\rho}(\lambda, z) = \int_0^\infty \rho(R', z) J_0(\lambda R') R' dR', \quad (35)$$

while the integration lower limits a and b are constants, and $F_1(\lambda)$ and $F_2(\lambda)$ are arbitrary functions of λ .

One can verify explicitly, by substituting (34) into (33), that this f does indeed solve the intended equation. However, it now looks as though we have got a problem, since the solution involves naked factors of $e^{\lambda z}$ and $e^{-\lambda z}$. These appear multiplying F_1 and F_2 , and also multiplying the integrals in z' . Considering e.g. $F_1(\lambda)e^{-\lambda z}$, this blows up as $z \rightarrow -\infty$ for any non-zero value of F_1 . (Note the range of λ is from 0 to ∞ .) Thereafter there is an integration over λ which occurs in equation (31) but no subsequent integration over z , and hence the singularity will persist into the final answer for Φ . The only way out of this is if $F_1(\lambda)$ is strictly zero, and of course the same considerations apply to for $F_2(\lambda)$. This then looks bad for the $e^{\pm\lambda z}$ multiplying the integrals, except in this case there is a ‘get out’. This is that the integrals are functions of z as well as λ , via the upper limit of integration. In particular if we choose the lower limit of integration b to be $-\infty$ then the integral will tend to zero as $z \rightarrow -\infty$, thus potentially (depending on respective rates of convergence of the integral and the outside $e^{-\lambda z}$ factor) leading to a finite answer. Similarly, in the first integral we should let $a = +\infty$, since then as $z \rightarrow \infty$ it is possible that a finite answer can be obtained here as well.

With these values of a and b , and setting $F_1(\lambda)$ and $F_2(\lambda)$ to zero, we get

$$f(\lambda, z) = \frac{2\pi}{\lambda} \left(\int_z^\infty e^{-\lambda(z'-z)} \tilde{\rho}(\lambda, z') dz' + \int_{-\infty}^z e^{\lambda(z'-z)} \tilde{\rho}(\lambda, z') dz' \right), \quad (36)$$

which assembles to give

$$f(\lambda, z) = \frac{2\pi}{\lambda} \int_{-\infty}^\infty e^{-\lambda|z-z'|} \tilde{\rho}(\lambda, z') dz', \quad (37)$$

for which convergence is assured if $\tilde{\rho}$, and therefore ρ itself, behaves reasonably.

This is excellent for our purposes. We have now achieved the analogue of equation Eq. (25b), but with the bonus that we know it is only the *inhomogeneous* part of the Poisson equation, i.e. the density itself, that does the ‘sourcing’. All possible homogeneous contributions have been killed off by the requirement that there should not be explicit $e^{\pm\lambda z}$ type factors left in the final answer.

Note that if we wanted to move towards an explicit solution for Φ from this point, we could write the solution so far as the triple integral

$$-\Phi = \int_0^\infty \lambda' d\lambda' \int_{-\infty}^\infty dz' \int_0^\infty R' dR' \frac{2\pi}{\lambda'} e^{-\lambda'|z-z'|} \times \rho(R', z) J_0(\lambda' R') J_0(\lambda' R). \quad (38)$$

This looks forbidding, but in fact we can explicitly carry out the λ integral by using the Bessel function identity drawn attention to in the paper [32] by Cohl & Tohline, specifically their equation (14), which reads, using the current variables,

$$\int_0^\infty d\lambda' e^{-\lambda'|z-z'|} J_0(\lambda' R') J_0(\lambda' R) = \frac{Q_{-1/2}(\chi)}{\pi \sqrt{RR'}}. \quad (39)$$

Here $Q_{-1/2}(\chi)$ is a Legendre function of the second kind and

$$\chi = \frac{R^2 + R'^2 + (z - z')^2}{2RR'}. \quad (40)$$

Cohl & Tohline further say that this Legendre function is related to the complete elliptic integral of the first kind, K , via

$$Q_{-1/2}(\chi) = \mu K(\mu), \quad (41)$$

where

$$\mu \equiv \sqrt{\frac{2}{1+\chi}} = \sqrt{\frac{4RR'}{(R+R')^2 + (z-z')^2}}. \quad (42)$$

At this point, inserting these results into (38), we see we have recovered (12), with all factors agreeing exactly, hence we can declare this method of approach to be successful. This is of course not surprising as regards determining the potential from the density, where we are perfectly happy with the idea that adding in extra homogeneous solutions is prohibited by the boundary conditions, but we now show in Section VIC that exactly the same analysis leads to the same conclusion for the poloidal gravitomagnetic field.

C. Repeating the analysis for the poloidal field

So we pick up from equation (31), but this time in a version for the poloidal field ψ . We will, however, re-use f for the Hankel transform of this field, since then many of the above relations will look almost identical. The particular version of Hankel transform which works best in terms of substituting into the gravitomagnetic equations is

$$\psi(R, z) = \int_0^\infty f(\lambda', z) R J_1(\lambda' R) \lambda' d\lambda', \quad (43)$$

where we can see the function Rf is being transformed by a J_1 . The equation we are substituting into is

$$\frac{1}{r} \frac{\partial^2 \psi}{\partial r^2} - \frac{1}{r^2} \frac{\partial \psi}{\partial r} + \frac{1}{r} \frac{\partial^2 \psi}{\partial z^2} = -16\pi \rho v. \quad (44)$$

We now insert (43) into this, obtaining

$$\int_0^\infty \left(\frac{\partial^2 f}{\partial z^2} - \lambda'^2 f \right) J_1(\lambda' R) \lambda' d\lambda' \quad (45)$$

$$= -16\pi \rho(R, z) v(R, z).$$

Taking an inverse Hankel transform of each side then yields

$$\frac{\partial^2 f}{\partial z^2} - \lambda^2 f = \quad (46)$$

$$-16\pi \int_0^\infty \rho(R', z) v(R', z) J_1(\lambda R') R' dR'.$$

Again this is a linear equation for f which we can solve by the method of variation of parameters. The full solution this time is

$$f(\lambda, z) = F_1(\lambda) e^{-\lambda z} + F_2(\lambda) e^{\lambda z}$$

$$- \frac{8\pi}{\lambda} \left(e^{\lambda z} \int_a^z e^{-\lambda z'} \tilde{j}(\lambda, z') dz' \right. \quad (47)$$

$$\left. - e^{-\lambda z} \int_b^z e^{\lambda z'} \tilde{j}(\lambda, z') dz' \right),$$

where we have defined a ‘matter current’ $j = \rho v$ and \tilde{j} is its Hankel transform (using a J_1)

$$\tilde{j}(\lambda, z) = \int_0^\infty \rho(R', z) v(R', z) J_1(\lambda R') R' dR' \quad (48)$$

The arguments given before about what happens as $z \rightarrow \pm\infty$ go through in exactly the same way, and we can jump straight to the final answer for f which is now

$$f(\lambda, z) = \frac{8\pi}{\lambda} \int_{-\infty}^\infty e^{-\lambda|z-z'|} \tilde{j}(\lambda, z') dz'. \quad (49)$$

We thus recover Eq. (25b), except now we know that the \tilde{v} in this *has* to be the transform of the inhomogeneous source j , and cannot contain a free homogeneous component.

In the units used above, which have 1 kpc as the unit of length, then clearly the j or \tilde{j} terms will be of order 10^{-9} and hence far too small to give the GEM effects claimed in the approach of [20], or indeed the possible substantial modifications to rotation curves claimed to be allowable in [21].

If we wish to progress in the same way as in the potential case to getting an explicit integral expression for ψ , then this will need the analogue of (39) for J_1 's. This reads

$$\int_0^\infty d\lambda' e^{-\lambda'|z-z'|} J_1(\lambda' R') J_1(\lambda' R) \quad (50)$$

$$= \frac{1}{\pi \sqrt{RR'}} Q_{1/2}(\chi),$$

and according to equation (23) in [32] we have

$$Q_{1/2}(\chi) = \chi \mu K(\mu) - (1 + \chi) \mu E(\mu), \quad (51)$$

where χ and μ are as defined earlier in equations (40) and (42) and E is the complete elliptic integral of the second kind. Thus overall we will obtain

$$\psi(R, z) = 8 \int_{-\infty}^\infty dz' \int_0^\infty R' dR' \sqrt{\frac{R}{R'}} \rho(R', z) \quad (52)$$

$$\times v(R', z) (\chi \mu K(\mu) - (1 + \chi) \mu E(\mu)).$$

D. Thin disks

Finally, we should comment on the relation to the ‘thin disk’ approach used by [21]. If we assume that

$$\rho(R, z) = \sigma(R) \delta(z), \quad (53)$$

where $\sigma(R)$ is the surface density, and adopt the definition for the spectral function for the potential given in equation (18) of [21], i.e.

$$\tilde{\Phi}(\lambda) = 2\pi \int_0^\infty R' \sigma(R') J_0(R' \lambda) dR', \quad (54)$$

then our $\tilde{\rho}$ is given by (see equation (35) above):

$$\tilde{\rho}(\lambda, z) = \delta(z) \int_0^\infty \sigma(R') J_0(\lambda R') R' dR' \quad (55)$$

$$= \frac{1}{2\pi} \delta(z) \tilde{\Phi}(\lambda).$$

Hence our $f(\lambda, z)$ as given by equation (37) is

$$f(\lambda, z) = \frac{1}{\lambda} \tilde{\Phi}(\lambda) e^{-\lambda|z|}, \quad (56)$$

and so our expression for (minus) the potential in this case is

$$-\Phi(R, z) = \int_0^\infty f(\lambda', z) J_0(\lambda' R) \lambda' d\lambda' \quad (57)$$

$$= \int_0^\infty \tilde{\Phi}(\lambda') e^{-\lambda'|z|} J_0(\lambda' R) d\lambda',$$

which agrees with equation (16) of [21] up to an overall sign.

This shows that, unsurprisingly, we can reach the thin disk results of [21] starting from a non-singular distribution in the case of the potential and exactly the same will go through for the poloidal field, in the sense that the thin disk results, when done correctly, must show the same behaviour as the thick-disk ones, i.e. the behaviour is sourced only by the ‘matter current’ and extra homogeneous solutions are not allowed.

VII. CONCLUSIONS

We have investigated the recent claims in [20] that one need not consider modified gravity theories to explain flat rotation

curves, such as those observed in galaxies, without the need for dark matter, since such curves can be explained by gravitomagnetic effects in standard linearised GR. We have also considered the related effects obtained in [21], specifically substantial gravitomagnetic corrections to the rotation curve of a galactic toy-model which are put forward as possibly being impactful in galactic dynamics.

In [20] the convenient GEM formalism is adopted and, somewhat unusually, a galaxy is modeled as an axisymmetric, stationary, rotating, non-relativistic and pressureless ‘dust’ of stars, all of which follow circular orbits. This approach therefore identifies the bulk velocity distribution of the galaxy with the velocity of stars, thereby aiming to define a self-consistent pressureless model.

The resulting system of GEM field equations for the gravitational (gravitoelectric) potential Φ and the poloidal gravitomagnetic flux ψ , together with the radial and vertical equations of motion, are amenable to an order of magnitude analysis. Indeed, it is straightforward to show that gravitomagnetic effects on the circular velocity v of a star are $\mathcal{O}(10^{-6})$ smaller than the standard Newtonian (gravitoelectric) effects. Thus, as one might have expected, any modification of Newtonian galaxy rotation curves must be negligible. More importantly, we find that the assumption in the [20] model that all the vertical support necessary to maintain dynamical equilibrium arises from gravitomagnetic effects is impossible to satisfy; if one assumes the presence only of ordinary matter, the gravitomagnetic effects are $\mathcal{O}(10^{-6})$ too small to provide this support.

The above issues are obscured when various quantities are eliminated between the system of equations to arrive at the single key equation for v used by [20]. Nevertheless, to understand how [20] appears to arrive at a self-consistent pressureless model for a galaxy, we solve this key equation for v in the case of a galaxy having a MN density profile. This allows us to establish an intuition for the results by adopting a ‘dual track’ approach by performing an exact numerical integration and by developing an accurate analytic approximation.

Adopting the derived values of the mass, M , and semi-major and semi-minor axes, a and b , obtained by [20] in fitting rotation curve data for NGC 1560, we find that the resulting rotation curve depends only very weakly on the mass M . Moreover, we show that for larger values of M , the rotation curve becomes independent of M . In any case, if one compares the rotation curve for the fitted parameters with the corresponding standard Newtonian rotation curve, one finds that the effects of gravitomagnetism are to suppress the rotational velocity of test particles, not enhance them. Thus, although the rotation curve including gravitomagnetic effects has a shape closer to that observed, it requires more matter to be present than in the Newtonian case in order to explain a given rotation curve level, which exacerbates the missing matter problem.

Although the predicted rotation curve for the fitted aspect ratio $a/b = 0.373/0.3$ matches the observed one reasonably well, this aspect ratio is somewhat smaller than what would be inferred from observations of NGC 1560 in the visible, which

is close to $a/b = 0.7/0.3 \approx 2.33$. We show, however, that for aspect ratios $a/b > 2$, the predicted rotation curves are concave over their entire range, which does not match observations in any galaxy.

The most problematic issue, however, is that in order to provide the necessary vertical support to maintain dynamical equilibrium, the poloidal gravitomagnetic flux ψ must become singular at the origin and have extremely large values near to it. In particular, we show that ψ must be at least $\mathcal{O}(10^8)$ larger than expected from gravitomagnetic effects. This must occur because free-space solutions of the Poisson-like equation that determines ψ are being unwittingly included, but this is forbidden if one wishes to avoid the presence of singularities. Moreover, the large values of ψ contradict the linearised treatment implicit in the GEM formalism. Consequently, one may rule out the GEM model proposed by [20] as a means of explaining flat or rising galaxy rotation curves without the need for dark matter.

The involvement in [20] of free-space solutions to the Poisson-like equation that determines ψ then leads us naturally to consider [21] where (although the authors emphasise that more detailed analysis is needed) such solutions are deliberately employed. The fact that the methods of [21] lead to a dummy integration variable appearing on the outside of a putatively physical expression is already quite suggestive. In fact, when we try to faithfully generalise the proposed approach in [21] from the infinitesimal thin disk limit to an extended density profile, we find that the implications for galactic rotation curves are qualitatively different from those proposed in [21]. The orbital velocity above and below the equatorial plane is indeed determined by an ODE in the axial direction, but this ODE requires initial data which may as well be taken as the rotation curve in the plane itself. Thus, the formulation is entirely non-predictive outside the thin disk limit. Far more seriously, we show conclusively in both the thin and thick disk cases that the free-space solutions on which [21] relies *necessarily violate the gravitomagnetic boundary value problem at the equatorial plane*: they are inadmissible without a matter current there. We note that this objection is independent from the guaranteed existence of divergent regions in the solutions (which [21] notes may be tuned to large radii away from the galaxy). We conclude that (i) only the inhomogeneous parts of the GEM solutions may contribute to the rotation curve, and that (ii) they do so in a predictive manner, depending on the matter source currents. In the context of GEM, derived from GR without any infrared modification, we further conclude that these matter currents must after all include a substantial ‘dark’ component to be consistent with the observed phenomena.

ACKNOWLEDGMENTS

WEVB is grateful for the kind hospitality of Leiden University and the Lorentz Institute, and is supported by Girton College, Cambridge.

-
- [1] F. Lelli, S. S. McGaugh, and J. M. Schombert, *Astron. J.* **152**, 157 (2016), arXiv:1606.09251 [astro-ph.GA].
- [2] F. Lelli, S. S. McGaugh, J. M. Schombert, and M. S. Pawlowski, *ApJ* **836**, 152 (2017), arXiv:1610.08981 [astro-ph.GA].
- [3] P. Li, F. Lelli, S. McGaugh, and J. Schombert, *ApJS* **247**, 31 (2020), arXiv:2001.10538 [astro-ph.GA].
- [4] P. Salucci, *A&A Rev.* **27**, 2 (2019), arXiv:1811.08843 [astro-ph.GA].
- [5] V. C. Rubin and J. Ford, W. Kent, *ApJ* **159**, 379 (1970).
- [6] V. C. Rubin, J. Ford, W. K., and N. Thonnard, *ApJ* **225**, L107 (1978).
- [7] V. C. Rubin, J. Ford, W. K., and N. Thonnard, *ApJ* **238**, 471 (1980).
- [8] A. Bosma, *AJ* **86**, 1825 (1981).
- [9] T. S. van Albada, J. N. Bahcall, K. Begeman, and R. Sancisi, *ApJ* **295**, 305 (1985).
- [10] J. L. Feng, *Ann. Rev. Astron. Astrophys.* **48**, 495 (2010), arXiv:1003.0904 [astro-ph.CO].
- [11] A. Deur, *Phys. Lett. B* **676**, 21 (2009), arXiv:0901.4005 [astro-ph.CO].
- [12] A. Deur, *MNRAS* **438**, 1535 (2014), arXiv:1304.6932 [astro-ph.GA].
- [13] A. Deur, *Eur. Phys. J. C* **77**, 412 (2017), arXiv:1611.05515 [hep-ph].
- [14] A. Deur, *Eur. Phys. J. C* **79**, 883 (2019), arXiv:1709.02481 [astro-ph.CO].
- [15] A. Deur, C. Sargent, and B. Terzić, *Astrophys. J.* **896**, 94 (2020), arXiv:1909.00095 [astro-ph.GA].
- [16] A. Deur, *Eur. Phys. J. C* **81**, 213 (2021), arXiv:2004.05905 [astro-ph.GA].
- [17] A. Deur, *Phys. Lett. B* **820**, 136510 (2021), arXiv:2108.04649 [physics.gen-ph].
- [18] A. Deur, *Class. Quant. Grav.* **39**, 135003 (2022), arXiv:2203.02350 [gr-qc].
- [19] F. I. Cooperstock and S. Tieu, *Int. J. Mod. Phys. A* **22**, 2293 (2007), arXiv:astro-ph/0610370.
- [20] G. O. Ludwig, *European Physical Journal C* **81**, 186 (2021).
- [21] D. Astesiano and M. L. Ruggiero, *Phys. Rev. D* **106**, L121501 (2022), arXiv:2211.11815 [gr-qc].
- [22] L. Lehner, *Class. Quant. Grav.* **18**, R25 (2001), arXiv:gr-qc/0106072.
- [23] L. Lehner and F. Pretorius, *Ann. Rev. Astron. Astrophys.* **52**, 661 (2014), arXiv:1405.4840 [astro-ph.HE].
- [24] C. M. Will, “The parametrized post-Newtonian formalism,” in *Theory and Experiment in Gravitational Physics* (Cambridge University Press, 2018) p. 78–104, 2nd ed.
- [25] C. M. Will, “Metric theories of gravity and their post-Newtonian limits,” in *Theory and Experiment in Gravitational Physics* (Cambridge University Press, 2018) p. 105–128, 2nd ed.
- [26] W. E. V. Barker, M. P. Hobson, and A. N. Lasenby, (2020), manuscript in preparation.
- [27] M. Korzynski, *J. Phys. A* **40**, 7087 (2007).
- [28] L. Ciotti, *Astrophys. J.* **936**, 180 (2022), arXiv:2207.09736 [astro-ph.GA].
- [29] M. P. Hobson, G. P. Efstathiou, and A. N. Lasenby, *General relativity: An introduction for physicists* (Cambridge University Press, Cambridge, UK, 2006).
- [30] M. Miyamoto and R. Nagai, *Publ. Astron. Soc. Jap.* **27**, 533 (1975).
- [31] J. P. Wilson and C. J. S. Clarke, *Classical and Quantum Gravity* **13**, 2007 (1996).
- [32] H. S. Cohl and J. E. Tohline, *The Astrophysical Journal* **527**, 86 (1999).